Estimating Block Effective Permeability with Geostatistics and Power Averaging

Clayton Deutsch

Department of Applied Earth Sciences, Stanford University

ABSTRACT

The problem of estimating the effective vertical permeability in heterogeneous reservoirs is addressed. A binary type permeability distribution with spatial autocorrelation is used to model the sandstone and shale in a shaly sandstone reservoir. A power averaging process for the component permeabilities is assumed. The averaging power has been related to parameters that may be inferred in practical circumstances. The two proposed factors may be inferred from an indicator variogram describing the geometrical relationship between the shales and the sandstone matrix. If detailed information is available at an appropriate reservoir block scale, more precise approximations of the power of averaging may be made.

At this stage the proposed technique has been developed on simulated reservoirs. The simulations have been done with rigid statistical control so that the anisotropic nature of the shale heterogeneities may be captured. The actual block effective permeability (power of averaging) of the reservoir blocks is determined through steady state, single phase flow simulation. The reservoir units contain no more than 30% shale by volume and the emphasis has been on studying flow normal to the bedding plane. Improvements on the traditional geometric average for vertical permeability are immediately evident.
KEYWORDS: Permeability, Power Averaging, Geostatistics

INTRODUCTION

The important problem of scale averaging is one that is beginning to receive more attention. An "average" is a unique value that would describe a volume given a set of measurements based on smaller volumes contained within the larger volume.

When considering a heterogeneous medium such as a sandstone/shale reservoir many of the variables in question may be averaged arithmetically. The average porosity of a volume is simply the arithmetic average of the porosities of all the smaller volumes

that constitute it. In general the arithmetic averaging process applies to all variables such as saturations or volume/weight percentages of various phases.

There are other characteristics that are not additive. Absolute or relative permeability and capillary pressure are in this category. The average of variables such as these depend not only on the univariate distribution of the variable based on small elemental volumes, but the average is dependent on the complete spatial and multivariate distribution of the variable. The intrinsic meaning of these characteristics can be questioned at a very basic level. The meaning of permeability only becomes evident when one considers an externally applied pressure drop to a fixed spatial volume of rock/porous media. These variables describe fundamental characteristics of a rock/porous media when fluid is flowing in it. For this reason the problem of averaging from one scale (i.e., core) to another (i.e., reservoir simulation block) is important.

If there is a significant proportion of shale in a sandstone reservoir the impact of the low permeability shales may be appreciable. The shales will cause the effective permeability to be less than the arithmetic average of the component sandstone and shale permeabilities. The spatial distribution and continuity of the shales will determine how great this effect will be. If the shale bodies are continuous in the horizontal plane the vertical permeability may be quite different from the arithmetic average. In practice, the geometric average has been used for vertical permeability. In this paper the actual averaging process (averaging power) has been observed for simulated reservoir blocks. In each simulated reservoir block characteristics of the shale bodies are correlated to the averaging process observed.

The numerical simulation of an indicator grid and subsequent calculation of the associated effective permeability has been adapted from the procedure used by A. Desbarats (1986). Throughout this paper the term "simulation" refers jointly to the simulation of the indicator network and the flow simulation which provides the effective

permeability of the heterogenous media.

POWER AVERAGING FOR BLOCK EFFECTIVE PERMEABILITY

The power averaging formulation or the general mixture rule may be written for a two component shale sandstone system. If certain physically plausible conditions are met (Korvin, 1981) the power averaging formulation is the only possible functional form of the effective average of a composite material.

Some formulae that make use of a power averaging approach include the Wyllie "time-average equation" (Wyllie et al, 1956), Meese and Walther's "vugular carbonate formula" (Meese and Walther, 1967), (Tegland, 1970, Mateker, 1971) for the sound speed and effective attenuation in an alternating sequence of sand shale layers, and (Beck, 1976; Rzhevsky and Novik, 1971; Schon, 1971; Woodside and Messner, 1961; Grant and West, 1965; Pearce, et al., 1973; etc.) for the estimation of thermal and electric conductivityof fluid filled sedimentary rocks.

The effective permeability of a block composed of shale and sandstone may be written as a power average of the component permeabilities:

$$Ke = \left(p \cdot Ksh^{\omega} + (1-p) \cdot Kss^{\omega} \right)^{\frac{1}{\omega}} \quad \text{for some real } \omega, \quad \omega \neq 0. \tag{1}$$

$$Ke = Ksh^{p} \cdot Kss^{1-p}, \quad \omega = 0.$$

with:

Ke = Block Effective Permeability.

Ksh = Permeability of the shales.

Kss = Permeability of the sandstone.

p = Proportion (volume fraction) of shale.

ω = Power of averaging.

The averaging power (ω) is constrained by the upper and lower limits 1.0 and -1.0 corresponding to the arithmetic and harmonic averages respectively. The geometric

average is found at $\omega = 0$. The power averaging model is not subject to any *a priori* hypothesis that can be validated or refuted. It is simply a model allowing the problem of determining Ke to be shifted to the problem of determining ω.

Figure 1 shows how the averaging power affects the resulting effective permeability for a bimodal distribution of permeability (Ksh =0.1 *md* and Kss =1000.0 *md*). The traditional arithmetic, geometric, and harmonic averages are shown for reference. All possible effective permeability values may be expressed as a power average with the averaging power between -1.0 and 1.0.

It has been shown that a power averaging approach is feasible (Journel et al., 1986) and that the averaging power is approximately independent of the proportion of shale (for p less than 0.5). The dependence of the averaging power on easily inferred or measurable statistical properties of a heterogeneous media has been attempted in this study. There are clear connections between measures of connectivity, such as indicator correlation in the flow direction, and the power of averaging.

GEOSTATISTICAL APPROACH

The geostatistical approach to estimating the power of averaging will now be discussed. An indicator random function is defined so that the geometry of the shale heterogeneities may be described. For a three dimensional (3-d) grid an indicator is defined at each location as numerically equal to 1 if the location is in shale and 0 if not. The shale intrusions may be imagined as 3-d groupings of 1's.

The geometrical relationship of two different populations is to be captured in a limited number of summary statistics. The summary statistics should be easy to infer in real situations. In practice one does not have the well defined indicator grid that is available in numerical simulation. One may have well logs, core data, geophysical data, and possibly production data. In this study the emphasis has not been on developing a

method to predict the block effective permeability given the exact shale geometry. The interest has centered on predicting the power of averaging with parameters that may be inferred in practical circumstances. There is no doubt that if one can draw on all the information contained in an indicator network, the power of averaging could be inferred more accurately.

Consider a reservoir block as part of a larger statistically stationary volume (i.e., the reservoir). As suggested above, the volume may be described by a numerical indicator grid. The indicator variogram may be inferred from actual indicator data and/or from soft geological description and interpretation. It is this variogram that links the shale geometry to the averaging power. Rather than the overall variogram representative of the reservoir, a local model specific for each block would be preferred.

It is not the variogram directly that describes the ability of such a random field to flow fluid. Some measures of connectivity that are related to the variogram and that are specific for a particular block (i.e., statistically unique) are desired.

From this point forward we will concern ourselves with regular three dimensional grid networks that are described by an indicator network. Such a block is shown schematically in figure 2(note: the large reservoir block shown belongs to a larger reservoir not illustrated). In all subsequent mathematical elaboration the block will be described by finite sums of elemental sub-blocks.

GEOSTATISTICAL MODEL OF THE PERMEABILITY FIELD

The three dimensional reservoir blocks are made up of elemental sub-blocks that are either 100% shale or 100% sandstone. The permeability of the elemental sub-blocks may take one of two values, that of sandstone or that of shale. Consider the shale indicator random function $I(x)$ defined for each elemental sub-block centered at point x:

$$I(x) = 1 \text{ if } x \text{ is in shale}$$
$$= 0 \text{ if } x \text{ is in sandstone} \quad (2)$$

The complementary sandstone indicator random function $J(x)$ may be defined:

$$J(x) = 1 - I(x) \quad (3)$$

The indicator function $I(x)$ has the following first and second order moments:

$$E\{I(x)\} = p = \text{volume fraction of shale in the block}$$
$$Var\{I(x)\} = C(0) = p(1-p)$$
$$Cov\{I(x), I(x+h)\} = C(h) = p(1-p)\,\rho(h)$$
$$\gamma(h) = C(0) - C(h)$$

with $\rho(h)$ and $\gamma(h)$ being respectively the correlogram and variogram of the random function $I(x)$.

Given a 3-d indicator field it is necessary to extract some simple and easily predicted characteristics that would relate the 3-d configuration of shale to the ability of the field to flow fluid (effective permeability). Two evident factors would be a measure of spatial continuity along the flow lines and a measure of spatial continuity perpendicular to flow. As the spatial continuity of the shales in the flow direction increases the power of averaging would increase. Similarly, as the spatial continuity of the shales in the plane perpendicular to flow increases, the power of averaging would decrease. A method will now be proposed that determines two parameters that have the desired properties.

The two parameters proposed ($\overline{\rho}(L)$ and $\overline{\rho}(S)$) may be calculated experimentally given an indicator grid and a model for the variogram defining the larger stationary volume. The variogram is required to provide a range of correlation in each of the coordinate directions. Alternately these parameters may be calculated solely from the variogram model if the only information available is an inferred variogram model. It will be shown that these parameters may be used to predict the power of averaging.

The spatial variance of $I(x)$ along a length L representing the dimension of the block in one of the coordinate directions may be written. Consider L in the coordinate

direction x (ref. Journel and Huijbrects (1978) pp 67):

$$\overline{\gamma}_I(L,L) = \frac{1}{n_x^2} \sum_{i=1}^{i=n_x} \sum_{j=1}^{j=n_x} \gamma_I(x_i - x_j) \tag{4}$$

The ergodic limit of this spatial variance is the variance of $I(x)$ ie. $p(1-p)$. For a measure of the spatial continuity the influence of the proportion of shale should be filtered. Standardizing $\overline{\gamma}_I(L,L)$ to its ergodic limit the following continuity factor can be defined:

$$\overline{\rho}^*(L) = 1 - \frac{\overline{\gamma}_I(L,L)}{p(1-p)}, \qquad \epsilon\ [0,1] \tag{5}$$

Note that this is equivalent to the average correlogram for the flow length L (hence the $\overline{\rho}$ notation). As the continuity of the shales in a particular direction increases the $\overline{\rho}^*(L)$ will get closer to the upper limit (1.0), as the continuity of the shales in a direction becomes very low, or the block becomes very large, $\overline{\rho}^*(L)$ will approach the lower limit (0.0).

It is also desirable to have a measure of continuity that may be used for any size block. In the work that is done here all the block dimensions are relative to the variogram range. As the dimension of the block becomes large (ie. greater than the variogram range) $\overline{\rho}^*(L)$ will asymptotically approach zero. The lack of correlation at large distances will dominate the $\overline{\rho}^*(L)$ regardless of the short scale variogram structure.

What seems intuitively reasonable and is indeed the case, is that the correlation at small distances would be more important than the correlation at long distances. So in a situation where an experimental or actual measure of the spatial continuity is to be calculated a better estimate of $\overline{\rho}(L)$ would be weighted such that the short scale structure has more influence. For each lag distance h_l the average correlogram is defined as $\overline{\rho}(h_l)$. Appendix A illustrates the calculation of $\overline{\rho}(h_l)$ given an indicator network.

A weighted sum of each $\overline{\rho}(h_l)$ with appropriately chosen weights would have the

properties that are desired. A weighted sum of this form may be written:

$$\overline{\rho}(L) = \sum_{l=0}^{l=n_z-1} \lambda_l \, \overline{\rho}(h_l) \;, \quad \sum_{l=0}^{l=n_z-1} \lambda_l = 1 \tag{6}$$

A $\overline{\rho}(L)$ equal to that given in equation 5 would result if each λ_l is set to $\frac{1}{n_z}$.

It is considered that after double the variogram range the block effective permeability does not change. If we impose the condition that beyond two times the variogram range all the weights are set to zero, and that the weighting function will decrease linearly to zero at this point, the following weights may be assigned:

$$\begin{aligned} &\lambda_l = b_1 - b_2 h_l, \quad \text{all } h_l < 2a \\ &\quad a = \text{variogram range} \\ &\quad b_1, b_2 = \text{constants chosen such that } \sum_{l=0}^{l=n_z-1} \lambda_l = 1 \\ &\lambda_l = 0, \quad h_l > 2a \end{aligned} \tag{7}$$

This system of weights is more justified than the unweighted average that is implicitly assumed in equation 5. In actual network simulations it has been observed that the correlations $\rho(h_l)$ at small lags h_l are more influential than those at larger lags. Also the weighted $\overline{\rho}(L)$ may be used to predict the power of averaging more precisely than the unweighted $\overline{\rho}(L)$.

A measure of the spatial continuity of $I(x)$ in the plane perpendicular to flow may be similarly calculated The plane perpendicular to flow will be denoted S. If the flow is vertical (z-direction) the x-y plane will be S. If horizontal flow (in the x-direction) is being considered S will be the y-z plane.

In the numerical modelling of the fluid flow there is no flow in any diagonal directions (except stepwise). For this reason the calculation of $\overline{\rho}(S)$ is essentially a sum of the $\overline{\rho}$ in the two directions defining S. If one was considering vertical flow ($S \bigcup x, y$):

$$\overline{\rho}(S) = \alpha \cdot \sum_{l=0}^{l=n_x-1} \lambda'_l \overline{\rho}(h_l) + (1-\alpha) \cdot \sum_{l=0}^{l=n_y-1} \hat{\lambda}_l \overline{\rho}(h_l) \quad \text{,with:} \tag{8}$$

$$\sum_{l=0}^{l=n_x-1} \lambda'_l = \sum_{l=0}^{l=n_y-1} \hat{\lambda}_l = 1.0 \quad \text{,and:}$$

$$\alpha = \frac{L_x}{L_x + L_y}$$

The weights λ'_l and $\hat{\lambda}_l$ are determined in an identical fashion to λ_i given in equation 7. The expected variogram range in the x and y directions need not be the same. The weight α is introduced to correct for unequal L_x and L_y. It is important to note that if either L_x or L_y is greater than two times the variogram range they should be reset to $2 \cdot a$ for the calculation of α. This is equivalent to calculating $\overline{\rho}(S)$ by summing the contributing $\overline{\rho}(h_l)$ for all lags h_l in the x and y directions.

Up to this point the actual connection between $\overline{\rho}(L)$, $\overline{\rho}(S)$ and ω has not been discussed. The $\overline{\rho}$ terms may be calculated if a variogram model and a block size is provided. This relationship is discussed next. The connection between experimentally calculated $\overline{\rho}$ terms and the averaging power is then discussed in detail.

DEVELOPMENT OF $\overline{\rho}$ FOR AN EXPONENTIAL VARIOGRAM

Given a variogram model and a block of fixed dimensions it is possible to calculate what $\overline{\rho}(L)$ and $\overline{\rho}(S)$ will be analytically. This has been done for the exponential variogram model with no nugget effect: $\gamma(h) = 1 - e^{\left(\frac{-3h}{a}\right)}$, with practical range a.

Figure three shows how $\overline{\rho}(L)$ will change as a function of the dimensionless block length. The analytical expression for $\overline{\rho}(L)$ as a function of the dimensionless block size is given in appendix A. If the block cross section is square (with respect to an isotropic variogram range) the $\overline{\rho}(L)$ for the length of one side will give $\overline{\rho}(S)$. If this is not the case one could read the $\overline{\rho}$ corresponding to the dimensionless block length in each direction and combine the two arithmetically (consider the weight α given in equation 8).

The $\overline{\rho}$ terms will decrease to around 0.276 as the size of the block exceeds two times the variogram range.

TESTING AND IMPLEMENTATION

In the following sections the research steps and results will be outlined. The standardized block model is as follows:

The dimensions of the simulated reservoir blocks have been expressed in terms of the variogram range in the three coordinate directions. It has been assumed that there is a finite range for $\gamma_I(h)$ and that it will isotropic in the horizontal plane. There will be a geometric anisotropy with the vertical range less than the horizontal range. The discretization is expressed as the number of points that describe the variogram range. For example: if the variogram range in a particular direction is 15 m (ie. $a_x = 15$ m), and the block size L_x is 30 m with sub-blocks each 3 m (d_x). The block length given will be $2 \cdot a_x$ and the number of discretization points will be presented as 5.

A constant shale permeability (Ksh) of 0.1 md, and sandstone permeability (Kss) of 1000 md has been used throughout. An exponential variogram model with a vertical to horizontal anisotropy 1/15 has been considered for the variogram $\gamma_I(h)$:

$$\gamma_I(h) = 1 - e^{\left(\frac{-3h'}{a}\right)} \tag{9}$$

$$h' = \sqrt{h_x^2 + h_y^2 + (15 \cdot h_z^2)}$$

h_x, h_y, h_z = rectangular coordinates of the vector h.

The geometrical anisotropy of 1/15 implies that the range of correlation in the vertical direction is one fifteenth of the horizontal range of correlation.

The study proceeded as follows:

1. A reservoir block filled in with a (0-1) network of elemental sub-blocks was

simulated 4000 times with the volume proportion of shale varying from 2.5% to 32.5%. Each simulation yields an effective block vertical permeability. The averaging power that would identify the block effective permeability was then calculated by numerical means knowing the proportion of shale.

2. For some of the actual grid networks used, the grid was plotted in a series of cross sections. Knowing the power of averaging associated with each grid, a visual inspection was made so that the reason for the differences in ω could be explained. All of the simulations considered for this particular exercise were at a constant proportion of shale.

3. The corresponding $\overline{p}(L)$ and $\overline{p}(S)$ (equations 6 and 8) were calculated. Recall that these parameters could be inferred in practical situations.

4. A detailed regression study directed toward the estimation of ω from $\overline{p}(L)$ and $\overline{p}(S)$ was performed.

A large number of simulations were initially performed so that the dependence of ω on p, $\overline{p}^*(L)$, and $\overline{p}^*(S)$ could be evaluated. Only the case of vertical flow was considered. The block size was $0.8 \cdot a_x$ by $0.8 \cdot a_y$ by $1.5 \cdot a_z$, with a discretization of 5 by 5 by 10. The conjecture that ω and p are approximately uncorrelated was found to be valid. The correlation between ω and p for the 4000 runs was found to be as 0.07.

The equal weighted $\overline{p}$ terms were retained in the simulation runs. As expected, a positive correlation existed between ω and $\overline{p}^*(L)$ and a negative correlation existed between ω and $\overline{p}^*(S)$. However, a great deal of scatter was observed. Figures 4 and 5 illustrate this. Instead of plotting a scattergram with thousands of points the median and quartiles of ω based on prediction within small classes of $\overline{p}^*$ are presented. The scattergram of ω versus $\overline{p}^*(L)$ as well as the figure showing the median and quartiles is included on figure 4. This allows one to compare the actual scatter to the measure of

scatter indicated by the median and quartile lines. Presenting the results in this manner is consistent with the ultimate objective of having parameters that will predict an ω.

A poor correlation exists between ω and the $\overline{\rho}^*$ terms. The correlation between ω and $\overline{\rho}^*(L)$ is 0.46, and the correlation between ω and $\overline{\rho}^*(S)$ is -0.21. Recall however that the power of averaging for vertical flow is, in practice, taken as zero which corresponds to the geometric average. From figures 4 and 5 the possibility of improving on this traditional approach can be appreciated. This led to the next step where the actual indicator grid was drawn to see if a relationship existed between ω and the geometry of the shale bodies that could be identified by visual inspection.

After inspection of the actual geometry of shale bodies a significant although not surprising observation was made. The major factor contributing to the flow performance of a heterogenous block is the fraction of the cross section perpendicular to flow, for all sections, that has no shale obstacles. However, this fractional area is not a parameter that would be predictable in an unaccessible hydrocarbon reservoir, thus its study has not been pursued further.

Upon a detailed look at the $\overline{\rho}(h_l)$ terms for various lag distances h_l it was noticed that ω was more highly correlated to the $\overline{\rho}(h_l)$ terms for small h_l. It was also evident that this correlation dropped off in a linear fashion to near zero between 1 and 2 times the variogram range. The block effective permeability stabilizes if the length of the block exceeds double the variogram range. On the basis of these observations the $\overline{\rho}$ terms defined in equations 7 and 8 were proposed. Important considerations for considering these $\overline{\rho}$ terms are:

- Their simplicity and the poss bility of estimating them in practice.
- They completely characterize the bivariate (two points) distribution of the shale bodies.

The equal weighted $\overline{\rho}$ and unequal weighted $\overline{\rho}$ were calculated for the grid networks in this stage. The correlation between ω and the weighted $\overline{\rho}(L)$ is 0.81, a substantial improvement over the correlation between ω and the unweighted $\overline{\rho}^*(L)$=0.64. For $\overline{\rho}(S)$ both cases yielded a correlation of -0.2. In all runs subsequent to this, both sets of $\overline{\rho}$ terms have been calculated. It has been observed that the weighted $\overline{\rho}$ terms yield better results in all cases.

The validation of this approach has been carried out for the case of vertical flow. Various block sizes and degrees of discretization have been considered. In each set of test runs the relationship between the power of averaging and the experimentally calculated indicator correlation have been observed. The characteristics of the five test cases considered are given in table 1.

Five Test Cases Considered

(all distances are relative to the ranges of the variogram model (9))

Test Run	Lx	dx	Ly	dy	Lz	dz	size
Base Case	0.8	7.5	0.8	7.5	1.5	6.7	6x6x10
1. Discretization II	0.8	6.3	0.8	6.3	1.5	6.7	5x5x10
2. Small Block	0.4	12.5	0.4	12.5	2.0	5.0	5x5x10
3. Large Block	2.0	2.5	2.0	2.5	2.0	5.0	5x5x10
4. Large Block II	3.0	1.7	3.0	1.7	3.0	3.3	5x5x10

Table 1: Characteristics of the test cases considered.

For each case 500 simulations have been performed. The effective permeability (Ke), power of averaging (ω), proportion of shale (p), equal weighted $\overline{\rho}^*(L)$, weighted $\overline{\rho}(L)$, equal weighted $\overline{\rho}^*(S)$, and the weighted $\overline{\rho}(S)$ have been retained for each simulation. Some initial observations:

1. The power of averaging (ω) is independent of p in all cases.
2. The weighted $\overline{p}$ terms (ref. equations 6 and 8) are better correlated to ω than the equal weighted $\overline{p}^{*}$ terms in all cases.
3. The relationship between ω and $\overline{p}(L)$ does not depend on the block size or level of discretization.
4. A good approximation of ω may be made from regression using only $\overline{p}(L)$. The parameter $\overline{p}(S)$ does not assist in predicting ω except in extreme situations such as very high $\overline{p}(S)$.

Figure 6 shows the median lines for predicting omega on the basis of $\overline{p}(L)$ for all five test cases. All five cases were combined and the corresponding median and quartile lines are shown for prediction of ω by $\overline{p}(L)$ on figure 6. On figure 7 a plot of the median and quartile lines for prediction of ω by the equal weighted $\overline{p}^{*}(L)$ is also shown. The weighted $\overline{p}(L)$ may predict ω more accurately than an unequal weighted $\overline{p}^{*}(L)$.

On figure 8 the median lines for prediction of ω by $\overline{p}(S)$ are shown. The near horizontal nature of these lines and the scatter observed leaves little hope to use $\overline{p}(S)$ in confidently predicting ω. Figure 9 shows the median and quartile lines for all the simulations combined. A multiple linear regression has been used to estimate ω from both $\overline{p}(L)$ and $\overline{p}(S)$. The inclusion of $\overline{p}(S)$ increases only marginally the correlation from 0.694 to 0.704.

From the tests that have been carried out it is apparent that the averaging power may be predicted by $\overline{p}(L)$. The proportion of shale and the indicator correlation in the plane perpendicular to flow have no effect on ω except for large $\overline{p}(S)$ or large p. High $\overline{p}(S)$ would mean that $\overline{p}(L)$ would be low. This is the justification for the cut off; $\overline{p}(L) \geq 0.17$. Referring to figure 6 the following piecewise linear model ω was adopted:

$$\omega = 6.0\,\overline{p}(L) - 1.00, \qquad \overline{p}(L) \leq 0.17 \tag{10}$$

$$\omega = 0.9\,\overline{\rho}(L) - 0.13, \qquad \overline{\rho}(L) > 0.17$$

This relationship is for vertical flow and should not be extrapolated beyond $\overline{\rho}(L)=0.5$. To test this regression model a cross validiation of each run of the test cases has been done. For each run the effective permeability has been estimated successively by the model proposed above and a geometric average. The mean and variance of the relative error of estimation will give a measure of the bias and accuracy of each method, see table 2. The relative error is defined as the true permeability minus the estimated divided by the true permeability. The closer the mean of the relative error to zero the less biased the estimator. The lower the variance of the relative errors the more accurate the estimator.

	Relative Error			
Estimate	mean	variance	minimum	maximum
1. Geometric Average	-0.0093	62.29	-209.3	0.87
2. Power Average knowing $\overline{\rho}(L)$	-0.0062	0.28	-12.7	0.92

Table 2: Relative error statistics using a geometric average and the model proposed in equation 10.

It comes as no surprise that the power averaging technique performs better than the traditional geometric averaging. It is interesting to see that the geometric average is unbiased although not accurate. The constant power of averaging that would give no bias on the relative errors is $\omega = -0.0125$. This is close to the geometric average. The improvement made by using the proposed prediction technique is appreciable.

Figure 10 shows how the Ke predicted by the model (ref. equation 10) compares to the geometric average. The median Ke lines shown have been obtained from equation 10. For example: consider $\overline{\rho}(L) = 0.25$ since $0.25>0.17$ the second part of equation 10 would be used. An ω of 0.095 may be calculated. Knowing the proportion of shale (0.1

and 0.25 considered on figure 10) one may use equation 1 to calculate the effective permeability (531 *md* for $p = 0.10$ and 190 *md* for $p = 0.25$). This has been done for $\overline{\rho}(L) = 0.1$ to 0.5. The interquartile range has been plotted in the same way as the median lines. Two additional piecewise linear models have been fit to the upper and lower quartiles of figure 7.

Figure 11 shows a cross plot of the true and estimated block effective permeability considering a geometric averagfe and a power average knowing $\overline{\rho}(L)$. All the test cases are shown. The bias and accuracy are better for the case of power averaging. However, the $\overline{\rho}(L)$ is never known exactly. This would cause the prediction to be less accurate than what is shown of figure 11b.

Two important problems must now be addressed; that of inferring $\overline{\rho}(L)$, and how one would handle the more realistic case of a multimodal distribution of permeability.

MULTIMODAL PERMEABILITY DISTRIBUTION

No experimental research has yet been carried out on this question. The technique tentatively proposed here is a mere extension of the "solution" proposed for the bimodal case.

The multimodal or continuous distribution of permeability must be split into n_c modes or classes. At the limit each permeability datum could represent a class. The following generalization can then be made:

$$Ke = \left(\sum_{i=1}^{i=n_c} p_i \cdot K_i^{\omega} \right)^{\frac{1}{\omega}} \qquad (11)$$

with:

Ke = block effective permeability.

n_c = number of modes or classes.

p_i = volume fraction of class i in the block.

K_i = permeability (arithmetic average) of class i.

ω = power of averaging.

A pre-defined cut off would be applied to the permeability field to obtain an indicator network. From the calculation of a $\overline{\rho}(L)$ an ω could be estimated. Considering the traditional alternative of using a geometric average, more accurate estimates can be expected with reasonable application of this technique.

INFERENCE OF $\overline{\rho}(L)$ AND $\overline{\rho}(S)$

Up until this point the inference of actual $\overline{\rho}$ values has not been discussed. The basic requirement to infer the $\overline{\rho}$ terms is a variogram model. If experimental or actual $\overline{\rho}$ terms are to be determined more information is required.

The most accurate and reliable way to infer a variogram model is to have data at a reasonable scale. The scale and spacing of the data would have to be less than the range of correlation. A variogram inferred from an outcrop in the central Sahara (ref. Desbarats, 1986 quoted by Haldorsen et.al. 1985) was found to be fit by an exponential model with a 15 m isotropic range of correlation in the horizontal plane and a 1 m range of correlation in the vertical direction.

Outcrop data would provide the most direct means to determine appropriate variogram models. Close to some oil fields there may be outcroppings of the same sedimentary units. In northern Alberta (Canada) there is mining of oil sands which provides direct access to the sedimentary structure of oil bearing strata which is similar to that of nearby oil fields. It is known that some of these structures contain shale. In any case, a catalogue of variograms for specific depositional environments may be constructed. The appropriate variogram can then be selected on this basis if no other information is available.

Well logs would provide a vertical variogram. On the basis of the gamma ray, S.P.,

or more recently lithology logging (P_e), the down hole shale indicator variogram could be inferred. More precisely the $\overline{\rho}(L)$ in the vertical direction could be calculated. This would provide a method to estimate the averaging process for vertical permeability from well logging. Depending on the direction of the drill hole the averaging process in other directions may also be estimated.

CONCLUSIONS AND DISCUSSIONS

A power averaging process is assumed for the component permeabilities in a heterogeneous reservoir. It is shown that a weighted indicator correlation in the flow direction may be used to predict the power of averaging. The indicator correlation may be inferred in practice if detailed information such as appropriate well logs or outcrop data are available. The indicator correlation may also be inferred from structural hypotheses regarding the shale bodies and corresponding indicator variograms. The method has been developed for vertical flow. It is the author's opinion that this approach provides a tractable engineering approximation to the problem of estimating the block effective permeability in shaly sandstone reservoirs.

The actual implementation of this method would have to be done in steps. A power average with a constant power that is greater than zero for vertical flow is suggested as the first step. As more research is being done, confidence in the prediction of a more precise averaging power will lead to better estimates of effective permeability.

ACKNOWLEDGMENTS

The author is grateful to Dr. A.G. Journel for pioneering research on the power averaging approach and for advice and criticism throughout this study. Mr. A.J. Desbarats must also be thanked for the simulation software that was used.

This research was made possible through SCRF (Stanford Center for Reservoir Forecasting) funded by the Standard Oil Company.

REFERENCES

1. Beck, A.E. An Improved Method of computing the thermal conductivity of fluid filled sedimentary rocks, Geophysics, 41: 133-144 (1976)

2. Desbarats, A.J. Numerical Estimation of Effective Permeability in sand shale Formations. submitted to Water Resources, (1986)

3. Grant, F.S. and West, G.F., Interpretation Therory in Applied Geophysics. McGraw-Hill, New York,N.Y. (1965)

4. Haldorsen, H.H.. and Chang, D.M. Notes on stochastic shales: From outcrop to simulation model, in Proceed. of the NIPER "Reservoir Characterization Technical Conference", Dallas, May (1985)

5. Journel, A.G., Deutsch, C.V., and Desbarats, A.J. Power Averaging for Block Effective Permeability, SPE 15128, 56th California Regional Meeting of SPE, (1986)

6. Journel, A.G., and Isaaks, E.H. Conditional Indicator Simulation: Application to a Saskatchewan Uranium Deposit, in Math. Geol. 16(7), pp 685-718 (1984)

7. Journel, A.G., and Huijbrects, Ch.J. Mining Geostatistics, Academic Press, San Francisco, (1978)

8. Korvin, G.. Axiomatic Characterization of the General Mixture Rule, Geoexploration, 19:267-276 (1981)

9. Mateker, E.J.Jr., Lithologic predictions from seismic predictions. Oil Gas J. Nov 8, 1971 pp 96-100 (1971)

10. Meese, A.D. and Walther, H.C., An investigation of sonic velocities in vugular carbonates, 8th SPWLA Symp., Denver

11. Rzhevsky, V. and Novik, G., The Physics of Rocks, Mir Publishers, Moscow (1971)

12. Schon, J. Ein Beitrag zur Klassifizierung und Systematik petrophysikalischer

Parameter, Neue Bergbautechnik, 1: 2-10 (1971)

13. Tegland, E.R., Sand-shale ratio determination from seismic interval velocity. 23rd Ann. Midwestern Mtg., SEG, AAPG, Dallas (1970)

14. Warren, J.E , and Price, H.S. Flow in heterogenous porous media, SPEJ vol 1 pp 153-169 (1961)

15. Woodside, W. and Messmer, J.H., Thermal conductivity of porous media, II. Consolidated Rocks. J. Appl. Phys., 32: 1696-1706 (1961)

16. Wyllie, M.R.J., Gregory, A.R. and Gardner, L.W., Elastic wave velocities in heterogeneous and porous media, Geophysics, 21: 41-70 (1956)

APPENDIX A: CALCULATION OF $\overline{\rho}$

Given a 3-d network (ref. figure 1) filled in with a shale indicator realization (ref. equation 2) the parameters $\overline{\rho}(L)$ and $\overline{\rho}(S)$ are to be calculated. It is enough to develop the calculation of $\overline{\rho}$ for one coordinate direction only. For the plane perpendicular to flow, the weighted sum of the $\overline{\rho}$'s in the two orthogonal directions defining the plane perpendicular to flow (ref. equation 8), may be taken. The calculation of the $\overline{\rho}(L)$ in the vertical (z) direction will be shown.

$\overline{\rho}(L)$ is defined as:

$$\overline{\rho}(L) = \sum_{l=0}^{l=n_z-1} \lambda_l \cdot \overline{\rho}(h_l) \qquad (A.1)$$

The vector h_l is a vector in the z direction with a magnitude equal to an integer multiple of d_z ie $(l \cdot d_z)$. The non-centered covariance for each lag (h_l) is given by:

$$A(h_l) = \frac{1}{n_x \cdot n_y \cdot n_z} \sum_{i=1}^{i=n_x} \sum_{j=1}^{j=n_y} \sum_{k=1}^{k=n_z-l} I(x_i, y_j, z_k) \cdot I(x_i, y_j, z_{k+l}) \qquad (A.2)$$

The average correlogram for each lag distance is determined by centering the non-centered covariance and normalizing to its ergodic limit. Each $\overline{\rho}(h_l)$, $l = 0,...,n_z-1$, is

given by:

$$\overline{\rho}(h_l) = \frac{A(h_l) - p^2}{p(1-p)} \tag{A.3}$$

The weights λ_l decrease linearly with increasing h_l and become nought at 2 times the variogram range. The number of grid blocks within this distance will be denoted n_{2a}. It is possible that the block is smaller than this distance, in which case the lesser of n_z and n_{2a} is used in the following as n_o:

$$\lambda_l = \frac{\frac{-1}{n_{2a}} h_l + 1}{\sum_{i=0}^{i=n_o} (1.0 - \frac{1}{n_{2a}} h_i)} \tag{A.4}$$

This calculation of $\overline{\rho}(L)$ may be made for any size block and the $\overline{\rho}(L)$ will depend only on the short scale structure. Possibly, if the block size is large, there may be a larger range nested structure. If this is the case the effect of this additional structure will have to be evaluated.

If one considers a given variogram model and assumes an infinite discretization the $\overline{\rho}(L)$ in any direction may be calculated analytically as a function of the dimensionless block length. This has been done for the exponential variogram model with no nugget effect. The linear weighting makes the expression seem complicated. The derivation may be simply made if one considers an infinite discretization and a continuous weighting function. The following expression is found.

$$\overline{\rho}(L) = \left(\frac{2a}{2aL - \frac{L^2}{2}}\right)\cdot\left(-\frac{a}{3}e^{\frac{-3L}{a}} + \frac{a}{3}\right) - \left(\frac{1}{2aL - \frac{L^2}{2}}\right)\cdot\left(\frac{a^2}{9} - \frac{a}{3}Le^{\frac{-3L}{a}} - \frac{a^2}{9}e^{\frac{-3L}{a}}\right) \tag{A.5}$$

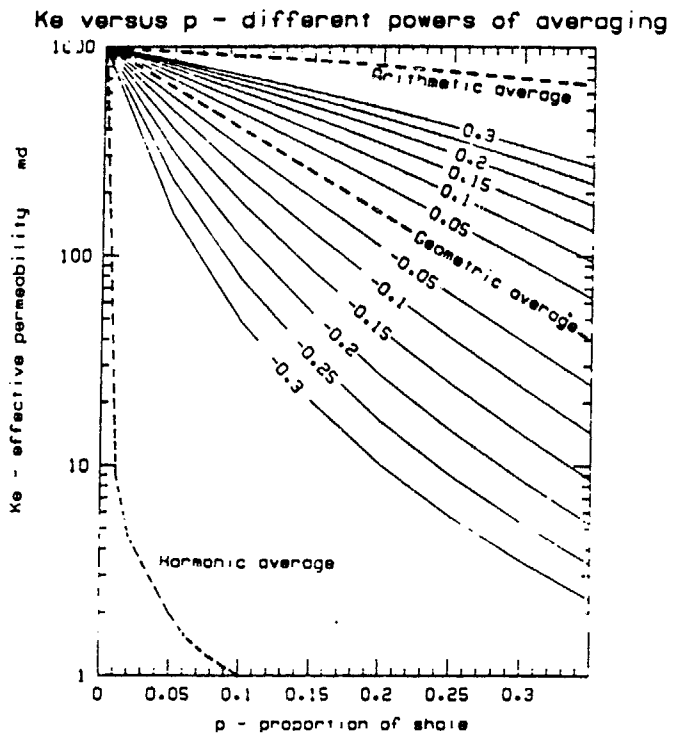

Figure 1: Effective permeability for different averaging powers.
A bimodal permeability distribution with $Ksh = 0.1$ md and $Kss = 1000$ md is used. The arithmetic, geometric, and harmonic averages are shown for reference.

Typical Discretized Reservoir Block

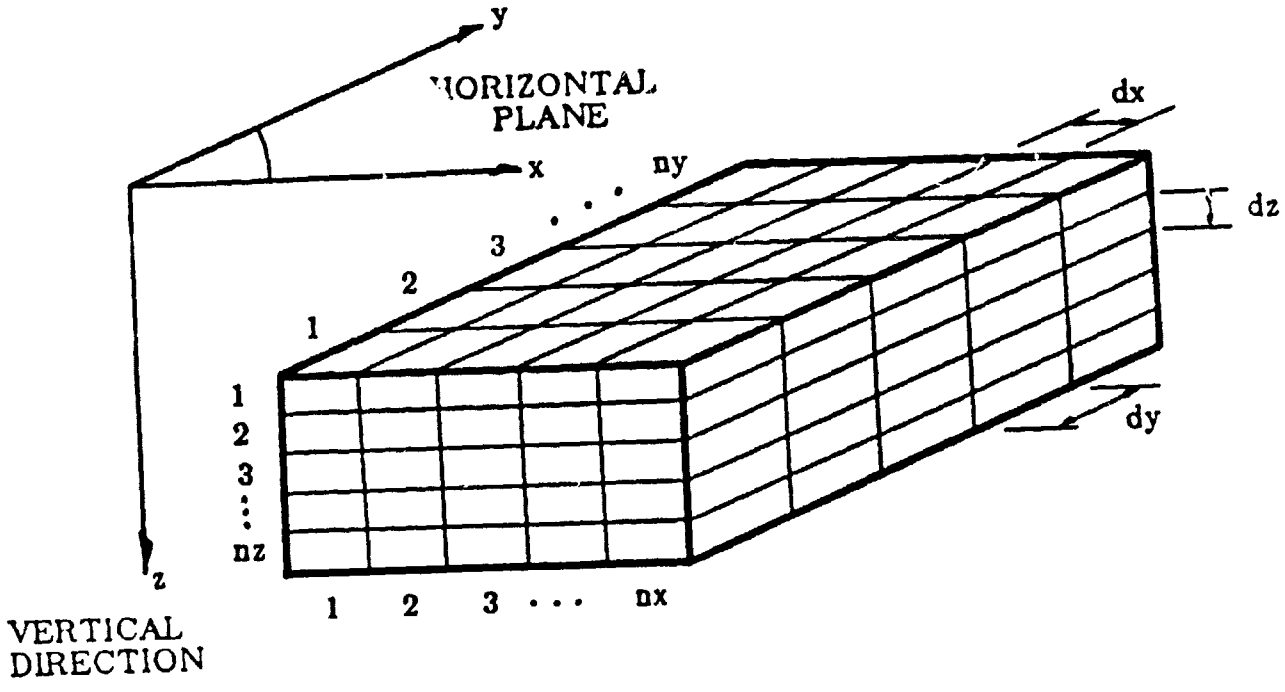

BLOCK SIZE:

$$Lx = dx \cdot nx$$

$$Ly = dy \cdot ny$$

$$Lz = dz \cdot nz$$

Figure 2: Typical Discretized Reservoir Block.

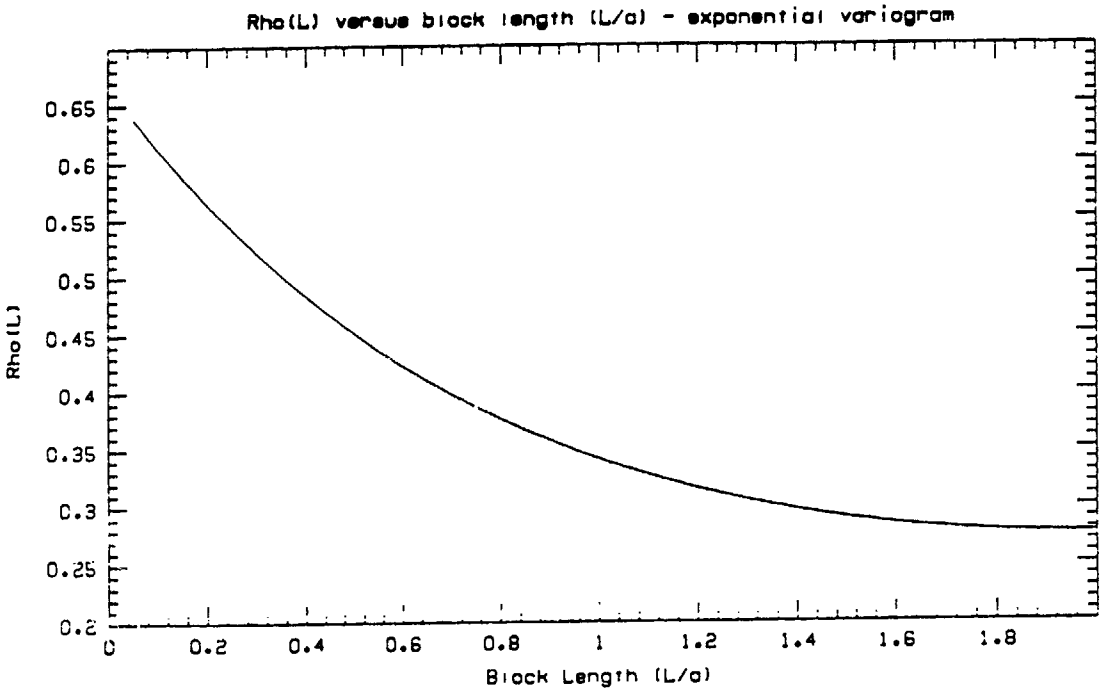

Figure 3: $\overline{\rho}(L)$ versus Dimensionless Block Length (L/a) for an exponential variogram model of range a.

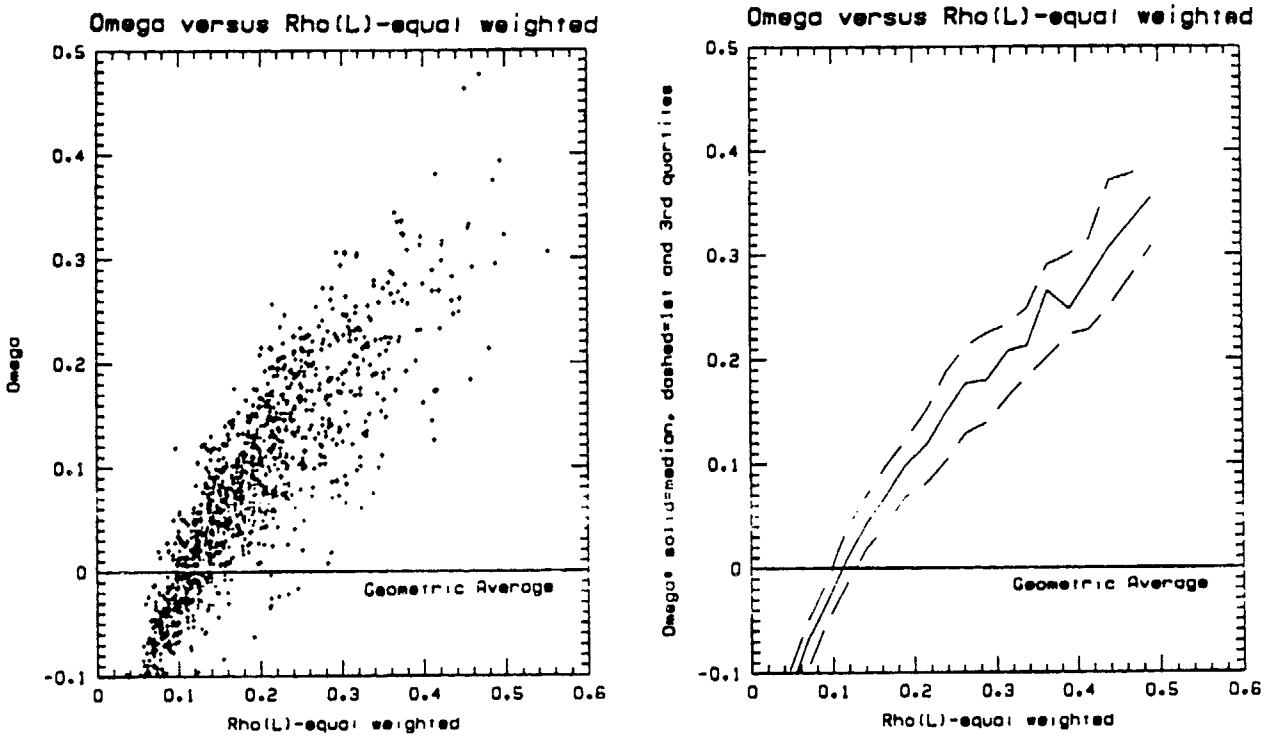

Figure 4: Power of Averaging (ω) versus $\overline{\rho}^{\omega}(L)$.
The scattergram and the corresponding plot of the median, first quartile, and third quartile lines, for the initial test runs, corresponding to the prediction of ω from small classes of $\overline{\rho}^{\omega}(L)$.

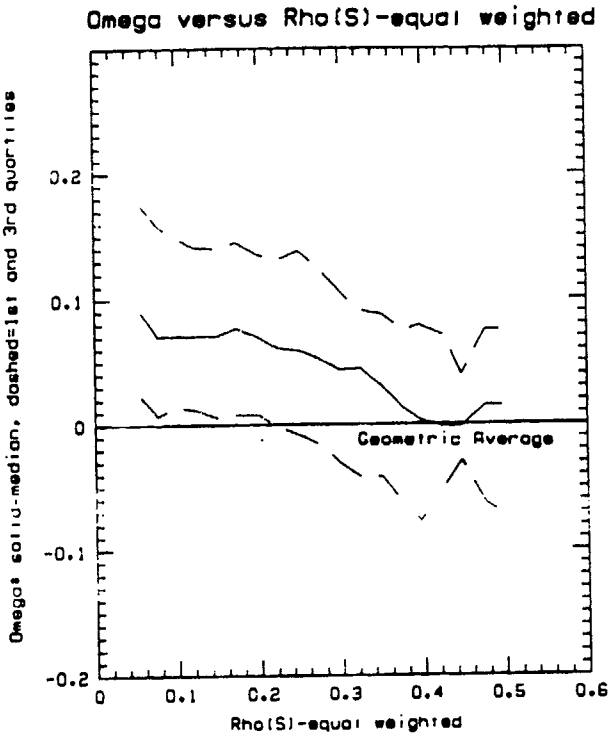

Figure 5: Power of Averaging (ω) versus $\overline{p}^{*}(S)$.
The median, first quartile, and third quartile lines plotted have been calculated from small classes of $\overline{p}^{*}(S)$, considering the prediction of ω from $\overline{p}^{*}(S)$.

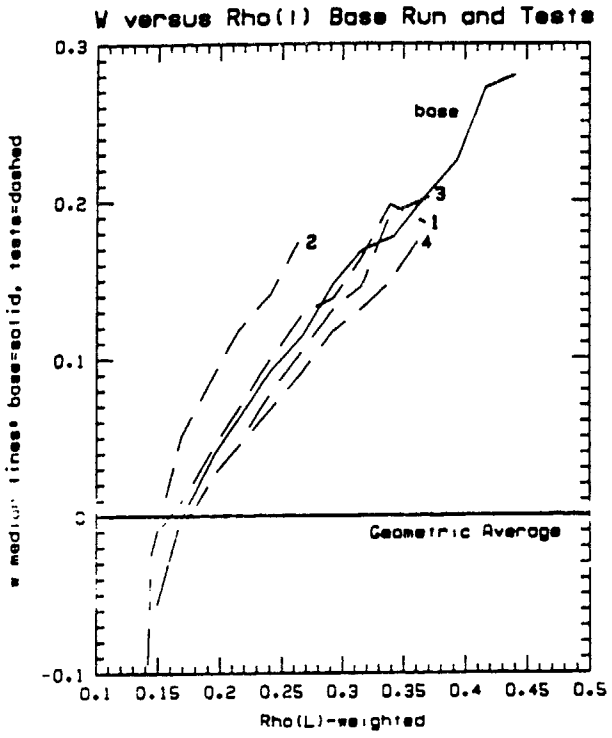

Figure 6: Power of averaging (ω) versus $\overline{\rho}(L)$.
Median lines for the four test runs and the base case are shown.

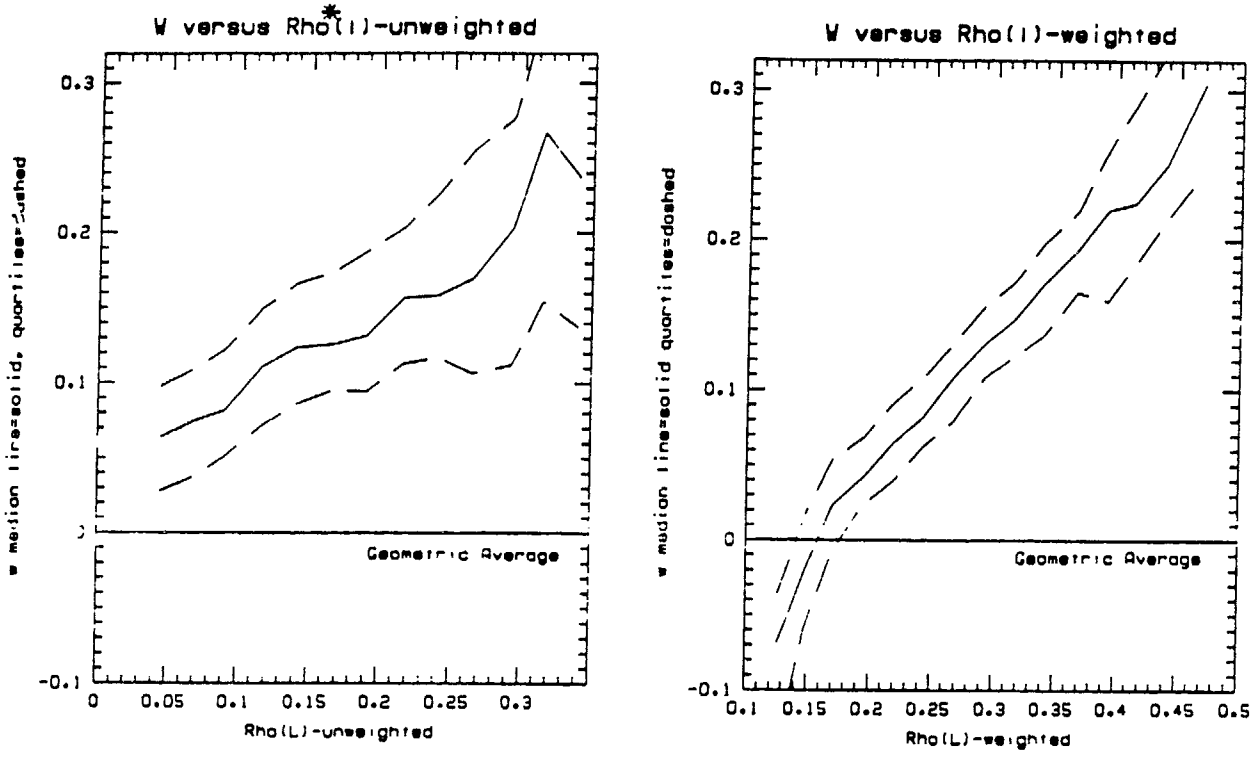

Figure 7: Power of Averaging (ω) versus $\overline{\rho}^{*}(L)$ and $\overline{\rho}(L)$.
All the test cases of table 1 have been combined to determine the median and quartiles of ω based on small classes of $\overline{\rho}(L)$. The 2500 effective ω's have been grouped per classes of either $\overline{\rho}^{*}(L)$ or $\overline{\rho}(L)$. The resulting class medians for ω were all positive in one case, and negative for low $\overline{\rho}(L)$ classes in the other case.

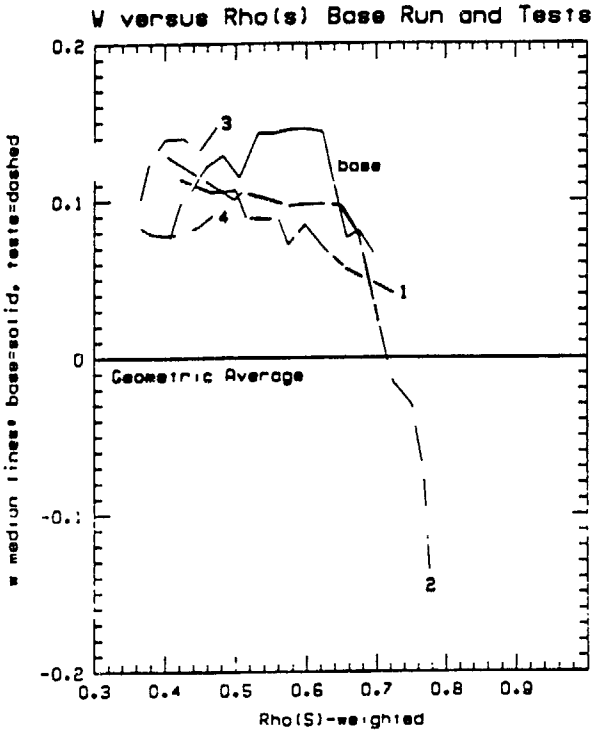

Figure 8: Power of averaging (ω) versus $\overline{\rho}(S)$.
Median lines for the four test runs and the base case are shown.

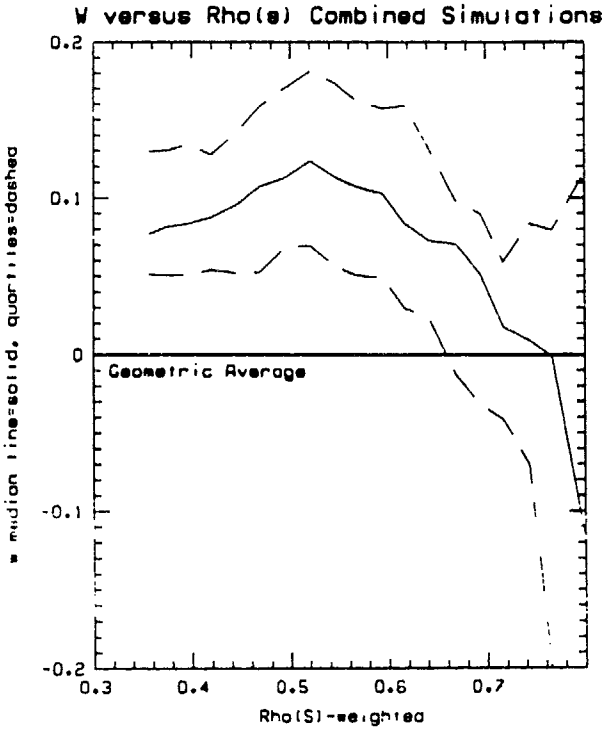

Figure 9: Power of Averaging (ω) versus $\overline{\rho}(S)$.
All the test data has been combined to determine the median and quartiles of ω based on small classes of $\overline{\rho}(S)$.

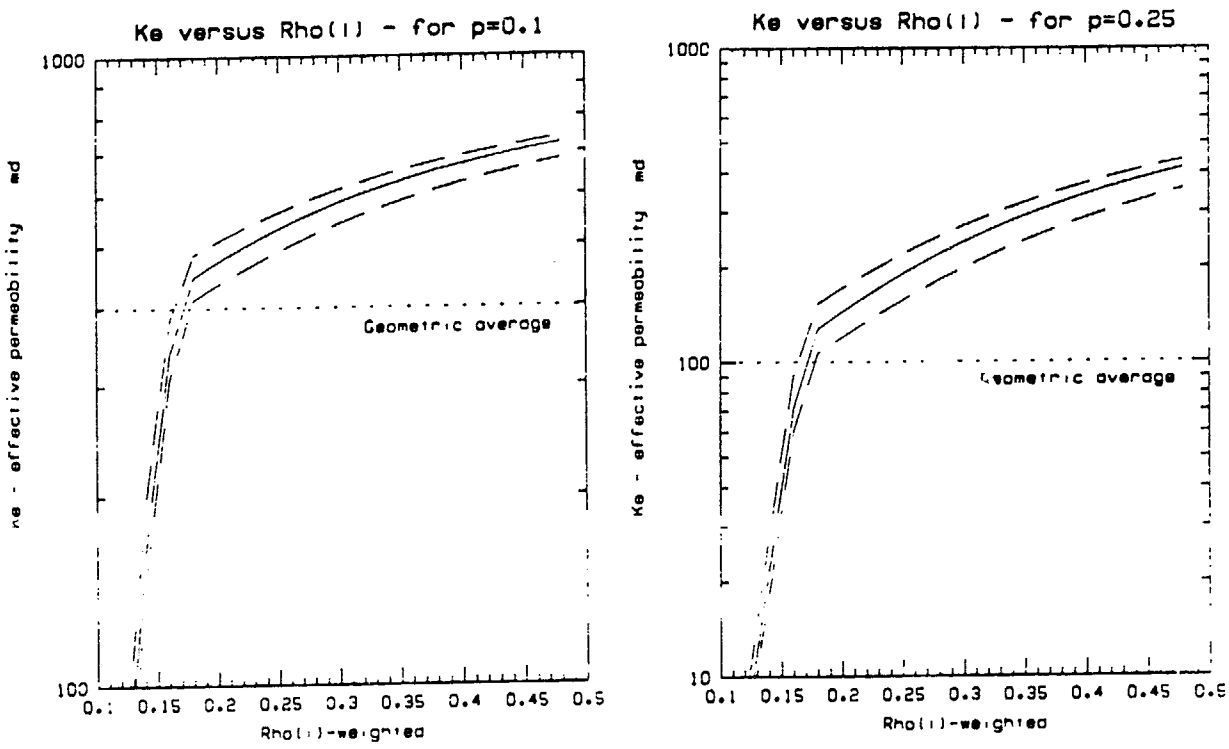

Figure 10: Estimating effective permeability from indicator statistics.
The averaging power is estimated from $\overline{\rho}(L)$, and the corresponding effective permeability is deduced. For a given volume proportion of shale, the figures give the distribution (median and interquartile range) of the resulting effective permeability estimates.

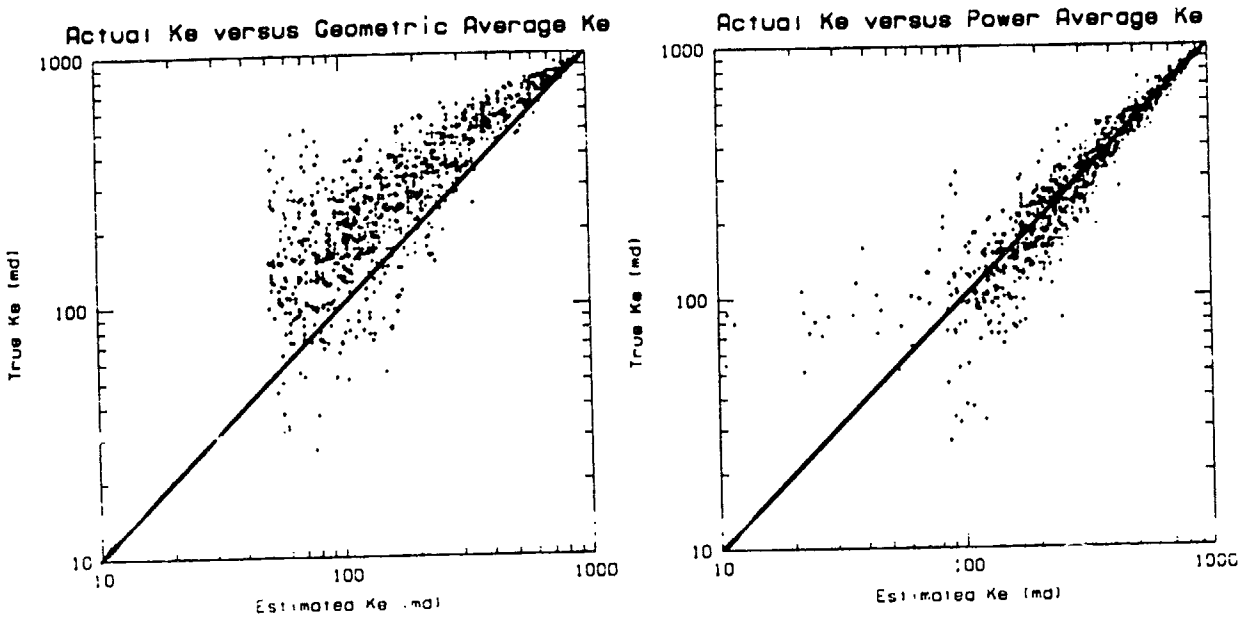

Figure 11: Actual Ke versus averaged Ke (Geometric average and Power average)
Note that the geometric average underestimates Ke for all ranges of estimated Ke. The power average is unbiased for all ranges of estimated Ke.